

Collective excitations of a quantized vortex in 3P_2 superfluids in neutron stars

Chandrasekhar Chatterjee,^{1,*} Mareike Haberichter,^{1,2,3,†} and Muneto Nitta^{1,‡}

¹*Department of Physics, and Research and Education Center for Natural Sciences,
Keio University, Hiyoshi 4-1-1, Yokohama, Kanagawa 223-8521, Japan*

²*Institut für Physik, Universität Oldenburg, Postfach 2503 D-26111 Oldenburg, Germany*

³*Department of Mathematics and Statistics, University of Massachusetts, Amherst, Massachusetts 01003-4515, USA*

(Dated: June 14, 2021)

We discuss collective excitations (both fundamental and solitonic excitations) of quantized superfluid vortices in neutron 3P_2 superfluids, which likely exist in high density neutron matter such as neutron stars. Besides the well-known Kelvin modes (translational zero modes), we find a gapfull mode whose low-energy description takes the simple form of a double sine-Gordon model. The associated kink solution and its effects on spontaneous magnetization inside the vortex core are analyzed in detail.

I. INTRODUCTION

The properties of high density nuclear matter are still not sufficiently understood. However, in recent years, neutron star (NS) observations began to place stronger restrictions [1–3] on the equation of state (EoS) of dense matter and to probe structure and composition of NS cores. Most valuable information into the state of their interiors came from the detections of pulsar glitches via pulsar timing measurements, optical and X-ray observations of cooling and accreting NSs and from neutrino emission measurements from proto-neutron stars. These observations provide evidence for superfluidity in the interiors of NSs [4].

The first direct evidence [5, 6] that the NS core should exist in a superfluid state has been reported in the study of the NS in the supernova remnant known as Cassiopeia A. It has been measured that Cassiopeia A's surface temperature has rapidly decreased from 2.12×10^6 K to 2.04×10^6 K. This pronounced drop in surface temperature can be naturally explained [5–7] if one assumes that neutrons have recently become superfluid in the NS core. As the neutrons combine to form Cooper pairs, a splash of neutrinos is emitted accelerating the NS cooling process. Another evidence for a superfluid NS core comes from the observation of pulsar glitches, which are sudden jumps in the NS rotation frequency. Glitches like the ones observed in the Crab and Velar pulsar can be explained by two main physical mechanism – either they are due to starquakes from the NS core [8, 9] or crust [10–12] or they are caused by the sudden unpinning and displacement of a large number of vortices [11–13] in the NS superfluid.

In the starquake glitch model [12, 14, 15], the glitches are caused by a sudden reduction in the moment of inertia of some solid component of the NS. For example, the differential rotation between the crust and the superfluid NS core can produce stresses [12] in the NS crust leading to crustquakes. The resulting crustquakes distort the star's shape and hence generate sudden jumps in the NS rotational frequency, seen as glitches. In contrast, in the pinned superfluid model angular momentum is suddenly transferred from the superfluid NS core to the non-superfluid crust via vortex unpinning, spinning it up. Neutron superfluid vortices can become pinned to nuclear clusters in the inner crust [11] or to magnetic flux tubes in the core [16]. This prevents angular momentum from being transferred to the NS crust. Hence, a differential rotation builds up between the NS core and crust. When this differential becomes large enough angular momentum is suddenly transferred from the core to the crust through the catastrophic unpinning of vortices, resulting in a sudden spin-up in the NS. Furthermore, the observed long time relaxation after glitches can be explained only by assuming the coexistence of normal and superfluid components [8, 10]. Therefore, understanding the properties of neutron superfluidity and the formation and dynamics of superfluid vortices can give us further insights into the evolution of NSs and their composition.

At the high density central part of NSs the neutron superfluidity is attributed to the 3P_2 pairing interaction [17–22] rather than to 1S_0 pairing familiar from the conventional BCS theory of superconductors. Analysis of nucleon-nucleon scattering data [18] shows that the transition from an isotropic 1S_0 superfluid to an anisotropic 3P_2 superfluid occurs at densities above 1.6×10^{14} g/cm³. The Ginzburg-Landau (GL) energy functional generalized for 3P_2 superfluids was developed in Refs. [21, 22] in the weak coupling limit. Note that the general GL free energy formally agrees with the angular momen-

* chandra@phys-h.keio.ac.jp

† mareike@math.umass.edu

‡ nitta@phys-h.keio.ac.jp

tum $l = 2$ GL functional solved by Mermin [23]; depending on the GL parameters, the ground state is in either nematic, ferromagnetic or cyclic phase. The ground states of 3P_2 superfluids in the weak coupling limit were found in Ref. [24] to be in the nematic phase in the absence of a magnetic field. They are continuously degenerated when we ignore the sixth order term and can be decomposed by unbroken $O(2)$, D_2 and D_4 symmetry groups into the uniaxial, D_2 - and D_4 -biaxial nematic phases, respectively. (This is also known from spin-2 spinor Bose-Einstein condensates, see Refs. [25, 26].) This degeneracy is lifted and the uniaxial nematic phase becomes the unique ground state once the sixth order term is taken into account. The ground states in the presence of a magnetic field were recently determined [27]; the ground state is in the uniaxial nematic phase for smaller magnetic fields relevant for ordinary NSs and in the D_2 - or D_4 -biaxial nematic phase for large magnetic field relevant for magnetars. Beyond the GL theory, the ground states in the (T, H) phase diagram have been obtained recently in the Bogoliubov-de Gennes (BdG) formalism [28]. The D_2 - and D_4 -biaxial nematic phases appear in lower T and H region and in higher T and H region, respectively. The phase boundary is of second order at higher temperature while it is of first order at lower temperature, and a tricritical point connects these boundaries. One of the most important results of the BdG formalism is that 3P_2 superfluids were found to be topological superfluids predicting gapless Majorana fermions on the surface [28]. The strong-coupling corrections to the 3P_2 NS matter GL free energy including spin-orbit and central forces were calculated in Ref. [29].

As phenomenological aspects relevant for NSs physics are concerned, 3P_2 superfluids provide new mechanisms for neutrino emission of dense neutron matter [30–39], explain the entrainment [40] of superconducting protons by rotating superfluid neutrons in NSs and offer possible explanations of the anomalously rapid cooling of NSs [5–7].

Since superfluids are rotating inside NSs, a large number ($\sim 10^{19}$) of superfluid vortices exist in their interior. The rich structure and magnetic properties of vortices emerging in the GL equations for 3P_2 superfluids were explored in Refs. [22, 27, 41–43]. 3P_2 vortices in NS matter turn out to be structurally different from their counterparts in 1S_0 superfluids. For example, different to 1S_0 vortices, 3P_2 vortices exhibit spontaneous magnetization in the vortex core region [27, 42]. For magnetic field strengths of orders of magnitude as they appear in magnetars, the ground state is in the D_4 -biaxial nematic phase, in which the first homotopy group π_1 is non-Abelian, thereby admitting non-Abelian (non-commutative) vortices which carry half-quantized circulation [43].

In this article, we study low-energy collective modes [(pseudo) moduli] and solitonic excitations of an integer vortex in a 3P_2 superfluid. By solving numerically the GL equation, we reconstruct the axially symmetric integer vortex solution in the absence of magnetic fields and sixth order terms. Because of the off-diagonal elements of the tensor order parameter, there exists spontaneous magnetization at the vortex core as described above. Here, we calculate the net magnetic moment per femtometer along vortex line to be one order less than the neutron magnetic moment. We then study collective modes in the presence of a single vortex. As usual, there are gapless (massless) Kelvin modes (translational moduli) due to the spontaneously broken translational symmetry in the presence of the vortex. In addition, the phase δ of the off-diagonal elements of the tensor order parameter gives rise to a gapfull (massive) mode. We construct the low-energy (long distance) effective free energy of this gapfull mode and find it is a double sine-Gordon model, consisting of the potential terms $\cos \delta$ and $\cos 2\delta$. For GL parameter values describing typical NSs, it allows only 2π kink solutions [44]. We find that the core magnetization of the vortex flips its direction at the kink.

The article is structured as follows. After introducing the GL free energy relevant for 3P_2 superfluids in the weak coupling limit, 3P_2 vortex solutions are constructed in Section II and their spontaneous magnetization in the vortex core region is evaluated. Then, in Section III, we discuss the effect of the parameter δ on the free energy density by writing down the associated effective free energy functional which takes the simple form of a double sine-Gordon model. The associated kink soliton solution is derived in Section IV. Finally, our conclusions and possible future lines of investigation are presented in Section V. To facilitate the reader to reproduce our numerical results, we add two appendices to this article. In Appendix A, we briefly review the GL theory for 3P_2 superfluid states and state all the parameter values used in our numerical simulations. We list explicitly all the vortex equations together with the imposed boundary conditions in Appendix C. Note that a detailed investigation of vortex structure and dynamics in the presence of nonzero external magnetic fields and higher order terms, in particular the inclusion of the sixth order term, will be published in a forthcoming paper.

II. GINZBURG-LANDAU DESCRIPTION OF VORTICES IN 3P_2 NEUTRON SUPERFLUIDS

In this section we discuss the GL free energy and determine the vortex configurations numerically. A discussion of spontaneous magnetization is included at the end of the section.

A. Ginzburg-Landau Free Energy

The GL free energy for the 3P_2 superfluidity was originally derived in Refs. [22, 42, 43, 45] by generalizing Gor'kov's procedure. In this case the original 1S_0 contact interaction was generalised to a 3P_2 contact interaction by introducing a derivative coupling. A short explanation of the derivation is given in Appendix A.

The tensorial order parameter $A_{\alpha i}$ transforms under the symmetry group as

$$A \rightarrow e^{i\theta} \mathbf{g} A \mathbf{g}^T, \quad \text{with} \quad e^{i\theta} \in U(1), \quad \text{and} \quad \mathbf{g} \in SO(3)_{L+S}. \quad (\text{II.1})$$

Here, $SO(3)_{L+S}$ is the diagonal subgroup of the full group $SO(3)_L \times SO(3)_S$ and is generated by the total angular momentum $J = L + S$.

The GL free energy density F can be written as a function of the tensor $A_{\mu i}$

$$F = \frac{1}{G} \int d^3\rho \left(F_{\text{grad}} + F_{2+4} + F_6 + F_H \right), \quad (\text{II.2})$$

where F_{grad} is the gradient term, F_{2+4} and F_6 [46] are the free energy densities up to fourth order and up to sixth order, respectively and F_H is the magnetic term. Here, we rescaled for later convenience the free energy functional by $G = 3\pi^2 / (m_n k_F^3) \approx 115.39 \text{ MeV fm}^5$ where k_F is the Fermi momentum and m_n represents the nucleon mass, see Appendix A for the numerical values of all model parameters. The free energy density contributions are explicitly given by

$$F_{\text{grad}} = K_1 \partial_i A_{\alpha j} \partial_i A_{\alpha j}^\dagger + K_2 \left(\partial_i A_{\alpha i} \partial_j A_{\alpha j}^\dagger + \partial_i A_{\alpha j} \partial_j A_{\alpha i}^\dagger \right), \quad (\text{II.3a})$$

$$F_{2+4} = \alpha \text{Tr} A A^\dagger + \beta \left[(\text{Tr} A A^\dagger)^2 - \text{Tr} A^2 A^{\dagger 2} \right], \quad (\text{II.3b})$$

$$\begin{aligned} F_6 = & \gamma_6 \left[-3 (\text{Tr} A A^\dagger) |\text{Tr} A A^\dagger|^2 + 4 (\text{Tr} A A^\dagger)^3 \right. \\ & + 12 (\text{Tr} A A^\dagger) \text{Tr} (A A^\dagger)^2 + 6 (\text{Tr} A A^\dagger) \text{Tr} (A^2 A^{\dagger 2}) \\ & + 8 \text{Tr} (A A^\dagger)^3 + 12 \text{Tr} [(A A^\dagger)^2 A^\dagger A] \\ & \left. - 12 \text{Tr} [A A^\dagger A^\dagger A^\dagger A A] - 12 \text{Tr} A A (\text{Tr} A A^\dagger A A) \right], \quad (\text{II.3c}) \end{aligned}$$

$$F_H = g'_H H^2 \text{Tr} (A A^\dagger) + g_H H_\alpha (A A^\dagger)_{\alpha\beta} H_\beta, \quad (\text{II.3d})$$

where H is the strength of the external magnetic field and we implicitly sum over repeated indices. Note that for simplicity, we set $g'_H = 0$ in Eq. (II.3d). In this paper we also neglect the sixth order term because of small values of γ_6 . Existence of nonzero γ_6 would make our system metastable, however we assume that small value of γ_6 would make the relaxation time much longer than the time scale of the system. All the following calculations will be performed in the weak coupling limit by considering only the excitations around the Fermi surface

[22, 45, 46]. In this limit, K_1 and K_2 in Eq. (II.3a) take the same value which is set to be K in the following. To simplify comparison with the works [22, 27, 42, 43], we fix the numerical values of the model parameters appearing in Eq. (II.3) as discussed in Appendix A and Table I.

As mentioned in the introduction, the ground state of the GL free energy is continuously degenerate in the absence of γ_6 and of external magnetic fields. Namely, the ground state order parameter in the cartesian basis can always be diagonalised using $SO(3)$ and $U(1)$ rotations to the form

$$A_{gs} = \sqrt{\frac{|\alpha|}{\beta(1+\eta^2+(1+\eta)^2)}} \begin{pmatrix} \eta & 0 & 0 \\ 0 & -(1+\eta) & 0 \\ 0 & 0 & 1 \end{pmatrix} \quad (\text{II.4})$$

where η is a dimensionless numerical parameter [27, 42, 47] taking values within the interval $-1 \leq \eta \leq -\frac{1}{2}$.

B. Vortex Configuration

Vortex configurations in the absence of a magnetic field and sixth order terms were first studied in Refs. [22, 41]. Since the order parameter is tensorial, we can choose a basis which diagonalizes the tensor at large distances from the vortex core. In Refs. [22, 41], the configuration in which the tensor is diagonalized in the cylindrical basis was considered. Later, this configuration was compared with the configuration in which the tensor is diagonalized in the Cartesian basis, and it was confirmed that the former gives the lowest energy configuration [27].

One interesting feature is that the vortex profile functions eventually choose asymptotically only one point among the whole degenerate ground state values. This means that the continuous degeneracy of the ground state, as mentioned in Eq. (II.4), is lifted [22, 27, 42] in the presence of a vortex at large distances.

In this subsection, we shall derive the equations of motion for the vortex profile functions using the following ansatz [27] for the order parameter of a vortex state

$$\begin{aligned} A^{(x,y,z)} &= \sqrt{\frac{|\alpha|}{6\beta}} R(\theta) A^{(\rho,\theta,z)} R^T(\theta) e^{i\theta}, \\ A^{(\rho,\theta,z)} &= \begin{pmatrix} f_1 & i g e^{i\delta} & 0 \\ i g e^{i\delta} & f_2 & 0 \\ 0 & 0 & -f_1 - f_2 \end{pmatrix}, \quad (\text{II.5}) \end{aligned}$$

where (ρ, θ, z) denote cylindrical coordinates and δ is a constant parameter. $A^{(x,y,z)}$ is the order parameters in the Cartesian basis and $A^{(\rho,\theta,z)}$ is the order parameters in the cylindrical

basis which are related by a rotation matrix R , given by

$$R(\theta) = \begin{pmatrix} \cos\theta & -\sin\theta & 0 \\ \sin\theta & \cos\theta & 0 \\ 0 & 0 & 1 \end{pmatrix}. \quad (\text{II.6})$$

For a brief motivation of the ansatz (II.5), we refer the reader to Appendix. B and Refs. [21, 22, 42, 46]. In Eq. (II.5), f_1 , f_2 and g are profile functions depending only on the radial coordinate ρ , and satisfying the boundary conditions

$$\begin{aligned} f_1 &\rightarrow -\sqrt{\frac{6}{2\eta^2 + 2\eta + 2}}\eta = 1.1116, \quad \text{as } \rho \rightarrow \infty \\ f_2 &\rightarrow \sqrt{\frac{3}{2}} \frac{2\eta + 2}{\sqrt{2\eta^2 + 2\eta + 2}} = 0.8841 \quad \text{as } \rho \rightarrow \infty, \\ g &\rightarrow 0 \quad \text{as } \rho \rightarrow \infty \\ f_1, f_2 &\rightarrow 0, \quad g \rightarrow 0 \quad \text{as } \rho \rightarrow 0, \end{aligned} \quad (\text{II.7})$$

where the dimensionless parameter η has a boundary value at spatial infinity determined by energy minimisation to be given by $\eta = 6 - \sqrt{43} \sim -0.557$ [22, 27, 41]; the continuous degeneracy of the ground state is lifted in the vortex background as described above. As the profile function g vanishes at the origin and at spatial infinity, it creates ring-shaped soliton solutions and in general one may replace g by $ge^{im\theta}$, where m denotes how many times the phase of g is twisted along the ring. Note that in Ref. [48] winding numbers that are locally defined in the core region were used to classify vortex-core structures in spin-1 Bose-Einstein condensates.

In Refs. [22, 27, 41] vortex solutions in 3P_2 superfluids have been constructed and analysed using the ansatz (II.5) for the order parameter of a vortex state. However, the effects of a non-zero phase parameter δ on the vortex structure have not been considered so far in the existing literature. Here, we introduce the constant phase δ in (II.5) to gain further insight into the collective excitations localised around a vortex. Around the vicinity of the vortex, one off-diagonal component was considered so far in the literature [22, 27, 41]. However, the authors only discussed the implications of a purely imaginary off-diagonal element. As a further generalisation of the vortex ansatz, we allow for real off-diagonal element contributions by introducing the non-zero phase δ in (II.5) as a minimal extension. This generalised ansatz is partly motivated by the idea that the phase might be a Nambu-Goldstone mode as it is often the case for solitons that a phase of a localised profile can be identified with a Nambu-Goldstone mode localised around the soliton. However, as we will learn in the following there exists a mass gap and therefore the phase δ cannot be considered as a Nambu-Goldstone mode.

Using the ansatz (II.5) we may rewrite the free energy (II.2) as

$$F = \int d^2\rho \frac{|\alpha|K}{6\beta G} \left\{ (t_1 + t_2) + \frac{\alpha}{K}t_3 + \frac{|\alpha|}{6K}t_4 \right\}, \quad (\text{II.9})$$

where the individual energy density contributions t_1, t_2, t_3 and t_4 take the following form

$$t_1 = 2(f_1'^2 + f_2'^2 + f_1'f_2' + g'^2) + \frac{1}{\rho^2} (4f_1^2 + 4f_2^2 - 2f_1f_2 + 10g^2 - 8(f_1 - f_2)g \cos \delta), \quad (\text{II.10a})$$

$$t_2 = 2(f_1'^2 + g'^2) + \frac{2}{\rho^2} \left\{ f_2^2 + 5g^2 + (f_1 - f_2)^2 - 2g(f_1 - f_2) \cos \delta + 4f_2g \cos \delta \right\} + \frac{1}{\rho} \left\{ -2(f_1' + f_2')g \cos \delta + 2(f_1 + f_2)g' \cos \delta + 2(f_1' + f_2')(f_1 - f_2) \right\},$$

$$t_3 = 2(f_1^2 + f_2^2 + f_1f_2 + g^2), \quad (\text{II.10b})$$

$$t_4 = 2f_1^4 + 4f_1^3f_2 + 6f_1^2f_2^2 + 4f_1f_2^3 + 2f_2^4 + \left\{ (6 + 2\cos 2\delta)f_1^2 + 4f_1f_2 + (6 + 2\cos 2\delta)f_2^2 + 4f_1f_2 \right\} g^2 + 2g^4. \quad (\text{II.10c})$$

Here the prime denotes the derivative with respect to ρ . For numerical calculations it is useful to rescale the radial coordinate by $\rho \rightarrow \tilde{\rho} = \rho/\xi$ where $1/\xi^2 = 12|\alpha|/K$ with ξ being the coherence length (~ 30 fm) and to change variables to $u = f_1 + f_2$ and $v = f_1 - f_2$. After rescaling and change of variables, the free energy (II.9) can be written as

$$F = \int d^2\tilde{\rho} \frac{2|\alpha|^2\xi^2}{G\beta} \left\{ (\tilde{t}_1 + \tilde{t}_2) + \frac{\alpha}{12|\alpha|}t_3 + \frac{1}{72}t_4 \right\} \quad (\text{II.11})$$

where the energy contributions read

$$\tilde{t}_1 = \frac{3}{2}u'^2 + \frac{1}{2}v'^2 + 2g'^2 + \frac{1}{\tilde{\rho}^2} \left(\frac{3}{2}u^2 + \frac{5}{2}v^2 + 10g^2 - 8vg \cos \delta \right), \quad (\text{II.12a})$$

$$\begin{aligned} \tilde{t}_2 &= \frac{1}{2}(u' + v')^2 + 2g'^2 + \frac{1}{\tilde{\rho}^2} \left(\frac{1}{2}u^2 + \frac{5}{2}v^2 - uv + 10g^2 \right. \\ &\quad \left. + 4g(u - 2v) \cos \delta \right) + \frac{1}{\tilde{\rho}} (2(ug' - gu') \cos \delta + 2u'v), \end{aligned} \quad (\text{II.12b})$$

$$t_3 = \frac{3}{2}u^2 + \frac{1}{2}v^2 + 2g^2, \quad (\text{II.12c})$$

$$t_4 = \frac{1}{8}(3u^2 + v^2)^2 + [(4u^2 + 2v^2) + (u^2 + v^2) \cos 2\delta] g^2 + 2g^4. \quad (\text{II.12d})$$

Here, the prime denotes the derivative with respect to $\tilde{\rho}$. Note that $\tilde{t}_1 = \xi^2 t_1(\rho) = t_1(\rho/\xi)$. In the following, we calculate the static vortex solution for $\delta = 0$. In the next section, the resulting vortex profile functions will be used to study perturbatively the effects of nonzero δ . We summarise the equations

of motion derived from the free energy functional (II.11) for vanishing δ together with the imposed boundary conditions in Appendix C.

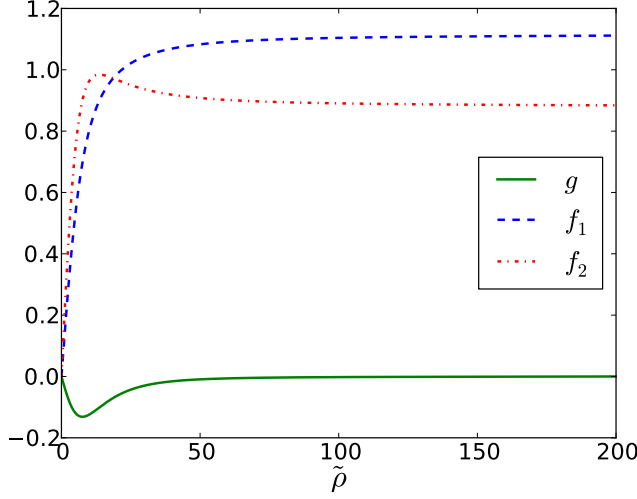


FIG. 1. We display the profile functions f_1 , f_2 and g for a vortex configuration of winding number one as a function of the distance $\tilde{\rho}$ from the vortex center. Here, the order parameter is expressed in the cylindrical basis ($n = 1$) and the vortex solution of lowest energy is found for the boundary value $\eta = -0.557$. Numerical results are shown for the case $m = 0$.

The obtained profile functions f_1 , f_2 and g are displayed in Fig. 1 as a function of the rescaled radial distance $\tilde{\rho}$ from the vortex center. To obtain solutions such as those shown in Fig. 1, we solve the equations of motion (C.1) with the boundary conditions stated in Eqs. (C.2) using a numerical relaxation method. The minimal energy solutions in the model (II.11) are constructed by solving the gradient flow equations with a crude initial guess (an approximation in terms of the hyperbolic tangents for the functions u and v and a gaussian curve approximation for the profile function g). The initial configurations are relaxed on a spatial grid with 2001 points and spacing $\Delta\tilde{\rho} = 0.1$.

3P_2 vortices are known to differ from their counterparts in 1S_0 superfluids by their nonzero magnetic moments [27, 42]. From the vortex profile functions displayed in Fig. 1, we can compute the resulting small spontaneous magnetization in the 3P_2 vortex core region.

The vortex magnetization is given in Refs. [27, 42] by

$$\mathbf{M} = \frac{\gamma_n \hbar}{2} \boldsymbol{\sigma}, \quad (\text{II.13})$$

where $\boldsymbol{\sigma}$ is computed as

$$\boldsymbol{\sigma} = C_m \frac{|\alpha|}{6\beta} g(\rho) [f_1(\rho) - f_2(\rho)] \cos \delta \hat{\mathbf{z}}. \quad (\text{II.14})$$

In the following, we take $\gamma_n = -1.83247172 \times 10^4 s^{-1} G^{-1}$ as experimental value for the neutron gyromagnetic ratio.

Here, $C_m = \frac{4}{9} N'(0) k_F^2$ and $N'(0) = m_n^2 / (2\pi^2 k_F)$ is the number density of states $N = m_n k / (2\pi^2)$ differentiated with respect to the energy $E = k^2 / 2m_n$ and evaluated at the Fermi surface $k = k_F$. For the numerical parameter values stated in Appendix A, $N'(0)$ takes the value $1.341 \times 10^{-5} \text{MeV}^{-2} \text{fm}^{-2}$ and C_m is computed to be $2.882 \times 10^{-5} \text{MeV}^{-2} \text{fm}^{-5}$. We display in Fig. 2 the resulting magnetization σ (II.14) for vanishing δ as a function of the rescaled distance $\tilde{\rho}$ from the vortex centre. The magnetization densities are evaluated using the vortex profile functions f_1 , f_2 and g plotted in Fig. 1. Substi-

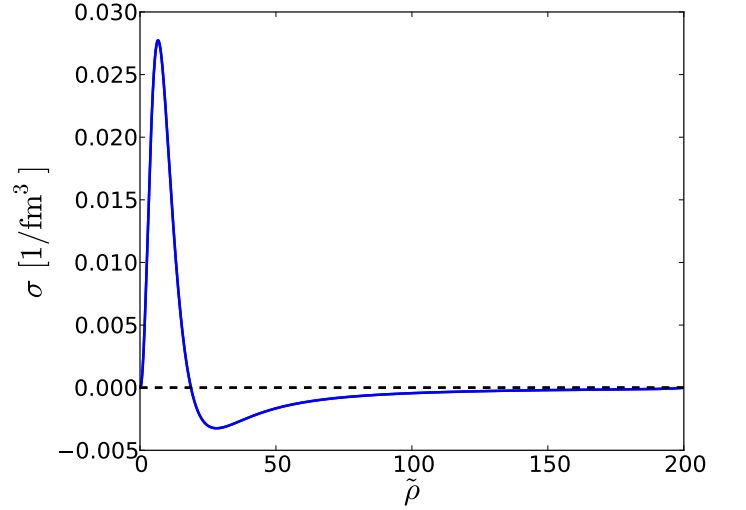


FIG. 2. Magnetization $\sigma(\tilde{\rho})$ for $\delta = 0$ plotted as a function of the rescaled distance $\tilde{\rho}$ from the vortex centre.

tuting the vortex profile functions computed for vanishing δ in (II.13), we can also find an estimate for the magnetization of the system as a function of δ . Integrating the magnetization (II.13) over the xy -plane gives the magnetic moment per unit length

$$\begin{aligned} m(z) &= \frac{\gamma_n \hbar}{2} 2\pi \xi^2 \int \tilde{\rho} d\tilde{\rho} \sigma(\tilde{\rho}) \\ &= C_m \frac{|\alpha|}{6\beta} \frac{\gamma_n \hbar}{2} 2\pi \xi^2 \int \tilde{\rho} d\tilde{\rho} g(\tilde{\rho}) (f_1(\tilde{\rho}) - f_2(\tilde{\rho})) \cos \delta \hat{\mathbf{z}}. \end{aligned} \quad (\text{II.15})$$

The integration in (II.15) can be performed numerically using the vortex profile function depicted in Fig. 1.

The integral is found to take the following value $2\pi \int \tilde{\rho} d\tilde{\rho} g(\tilde{\rho}) (f_1(\tilde{\rho}) - f_2(\tilde{\rho})) = -404.83$. Hence, for vanishing δ the magnetic moment per unit length is given by $m(z) \approx 4.196 \times 10^{-19} \text{MeV fm}^{-1} \text{G}^{-1} \approx 0.6 \times 10^{-27} \text{JT}^{-1} \text{fm}^{-1}$. Therefore, the magnetic moment of a 10 fm string is found to

be comparable to the neutron magnetic moment.

III. THE LONG DISTANCE EFFECTIVE DESCRIPTION OF FREE ENERGY OF A VORTEX

In this section we discuss the effective description of collective excitations along a vortex line by using the so-called moduli approximation, originally used for monopoles [49] and applied to various topological solitons, e. g. [50]. At large distances, superfluid vortices can be characterized by Kelvin modes. When orientating the vortex axis along the z -axis, these two moduli correspond to translations in the x - and y -direction. Physically these modes can be interpreted as the massless Nambu-Goldstone excitations generated from the spontaneous breaking of the translational symmetry [51, 52]. These modes are well studied in the literature of superfluids [53] and are not an issue of this paper.

In this article, we want to explore collective excitations localized around the vortex. We introduce a massive mode δ which may be important for understanding the spontaneous magnetization of the 3P_2 vortex. Interestingly, when we switch on the mode δ in Eq. (II.13), the spontaneous magnetization changes inside the vortex core.

In this article we solved the equations of motion by impos-

ing cylindrical symmetry, which makes the profile function independent of the z -coordinate. The parameter δ has been introduced as a constant phase in the off-diagonal element for a vortex solution in the xy -plane. As we know, the vortex profile functions eventually reach their ground state values (II.7) at large distances from the vortex core and $g(\rho)$ forms a concentric ring around the vortex. So $g(\rho)$ becomes practically zero outside the vortex, see Fig. 1. Therefore, we may treat δ as a collective coordinate (or a modulus) of a vortex and may take it as a function of z in the effective free energy functional. In principle, δ also depends on time but here we are not considering time dependence. In our case, δ is a slowly varying function of the z -coordinate.

The parameter δ depends on z and the z derivative of δ also contributes to the total effective energy. We insert the ansatz

$$A_{\delta}^{(\rho, \theta, z)} = e^{i\theta} \begin{pmatrix} f_1^0(\rho) & ig_0(\rho)e^{i\delta(z)} & 0 \\ ig_0(\rho)e^{i\delta(z)} & f_2^0(\rho) & 0 \\ 0 & 0 & -f_1^0 - f_2^0 \end{pmatrix} \quad (\text{III.1})$$

into the free energy functional (II.2) with the sixth order and magnetic term set to be zero and with the gradient and up to fourth order term given in Eqs. (II.3a) and (II.3b), respectively. With the ansatz (III.1) substituted into (II.2), the effective free energy takes the following form

$$F = \frac{4\alpha^2\xi^4}{\beta G} \int dz d^2\tilde{\rho} \left[\frac{1}{\xi^2} \left\{ \left(\frac{2g_0}{\tilde{\rho}^2} (u_0 - 4v_0) + \frac{1}{\tilde{\rho}} (u_0 g_0' - g_0 u_0') \right) (\cos \delta - 1) + \frac{g^2}{144} (u_0^2 + v_0^2) (\cos 2\delta - 1) \right\} + (\partial_z \delta)^2 g_0^2 \right], \quad (\text{III.2})$$

where f_1^0 , f_2^0 and g_0 are the vortex profile functions for zero δ , see Fig. 1. $u_0(\tilde{\rho})$ and $v_0(\tilde{\rho})$ are defined as $u_0 = f_1^0 + f_2^0$ and $v_0 = f_1^0 - f_2^0$, respectively. The rescaled radial distance $\tilde{\rho}$ is given by $\tilde{\rho} = \rho/\xi$, where ξ is the coherence length of the system. Eq. (III.2) can be expressed more neatly as,

$$F_{\text{eff}} = \int dz \frac{4\alpha^2\xi^4}{\beta G} \left[\frac{1}{\xi^2} \{ \lambda_1 (\cos \delta - 1) + \lambda_2 (\cos 2\delta - 1) \} + (\partial_z \delta)^2 \lambda_3 \right], \quad (\text{III.3})$$

where the coefficients are defined as

$$\lambda_1 = \int d^2\tilde{\rho} \left(\frac{2g_0}{\tilde{\rho}^2} (u_0 - 4v_0) + \frac{1}{\tilde{\rho}} (u_0 g_0' - g_0 u_0') \right), \quad (\text{III.4a})$$

$$\lambda_2 = \int d^2\tilde{\rho} \frac{g^2}{144} (u_0^2 + v_0^2), \quad (\text{III.4b})$$

$$\lambda_3 = \int d^2\tilde{\rho} \tilde{\rho} g_0^2. \quad (\text{III.4c})$$

The coefficients λ_1, λ_2 and λ_3 have been evaluated numerically to be given by

$$\lambda_1 = -4.889, \quad \lambda_2 = 0.411, \quad \lambda_3 = 17.748. \quad (\text{III.5})$$

Note that the signs and numerical values of the λ coefficients are very important in this work. The graph of the effective potential (III.3) should exhibit a bump at the bottom because of the negative sign of the λ_2 contribution. However,

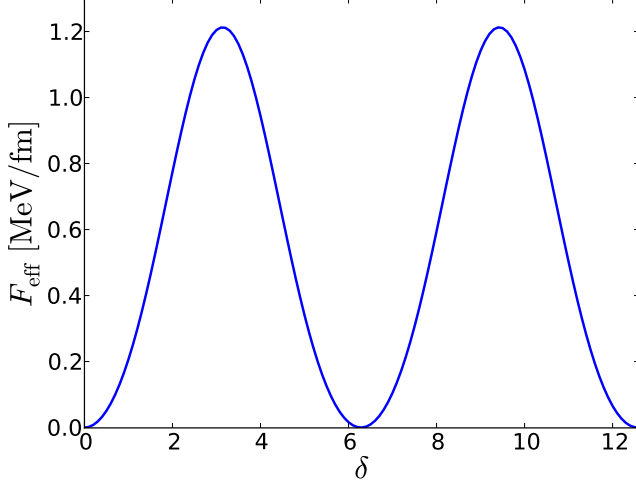


FIG. 3. We display the effective free energy potential F_{eff} (III.3) as a function of the δ parameter. We evaluate the free energy for the λ coefficients listed in Eq. (III.5). The GL parameters are given by $\alpha = -0.1$ and $\beta = 2.57664(\text{MeV fm})^{-2}$. The coherence length of the system is set to 30.3634fm . Note that the energy values are given in units of MeV fm^{-1} .

as can be seen from Fig. 3, the minima occur at $\delta = 2\pi n$ with n being an integer. To get any local extrema other than $n\pi$, δ has to satisfy the equation

$$\cos \delta = \frac{|\lambda_1|}{4\lambda_2}. \quad (\text{III.6})$$

It can be checked that the numerically evaluated λ values (III.5) yield $\frac{|\lambda_1|}{4\lambda_2} > 1$. Hence, the obtained λ coefficients do not support any other local minima or maxima. This finding supports our expansion of the system around $\delta = 0$.

IV. DOUBLE SINE-GORDON KINK SOLUTION ON A VORTEX

In the last section, we have derived the effective free energy functional (III.3) that describes the low-energy dynamics of the system along with other dynamical terms. Since in this article we are solely interested in time independent configurations, we discuss in the following the static solutions of the system. Note that the system (III.3) is known as the double sine-Gordon model. However, the potential graph shown in Fig. 3 almost agrees with the sine-Gordon case because of $|\lambda_2| \ll |\lambda_1|$, see Eq. (III.5). Here, we shall derive the kink solution and describe the physics behind the existence of the kink. We use the technique similar to Bogomol'nyi-Prasad-Sommerfield (BPS) monopoles [54, 55].

Let us rewrite the free energy (III.3) as,

$$F_{\text{eff}} = \frac{4\alpha^2|\lambda_1|\xi^2}{\beta G} \int dz \left[\left\{ (1 - \cos \delta) + \frac{\lambda}{2}(\cos 2\delta - 1) \right\} + \frac{\xi^2\lambda_3}{|\lambda_1|}(\partial_z \delta)^2 \right], \quad (\text{IV.1})$$

where $\lambda = \frac{2\lambda_2}{|\lambda_1|}$. The numerical value of λ is evaluated to be 0.168735. After rescaling z , the effective free energy in Eq. (IV.1) takes the form

$$F_{\text{eff}} = \frac{M_E}{2} \int d\zeta \left[\{2(1 - \cos \delta) + \lambda(\cos 2\delta - 1)\} + (\partial_\zeta \delta)^2 \right], \quad (\text{IV.2})$$

where $\zeta = \sqrt{\frac{|\lambda_1|}{2\lambda_3}} \frac{z}{\xi}$ and

$$M_E = \frac{4\alpha^2\xi^3\sqrt{2}|\lambda_1|\lambda_3}{\beta G}. \quad (\text{IV.3})$$

Although the second term in Eq. (IV.2) is not positive, the potential part of Eq. (IV.2) is positive definite. So, we can use the BPS technique to find the kink solution. To do that we write the F_{eff} as,

$$F_{\text{eff}} = \frac{M_E}{2} \int d\zeta \left[\left\{ \partial_\zeta \delta \pm \sqrt{2(1 - \cos \delta) + \lambda(\cos 2\delta - 1)} \right\}^2 + M_E \left| \partial_\zeta \delta \sqrt{2(1 - \cos \delta) + \lambda(\cos 2\delta - 1)} \right| \right] \quad (\text{IV.4})$$

Then F_{eff} satisfy the inequality

$$F_{\text{eff}} \geq E_{\text{BPS}} = M_E \left| \int d\zeta \partial_\zeta \delta \sqrt{2(1 - \cos \delta) + \lambda(\cos 2\delta - 1)} \right|. \quad (\text{IV.5})$$

The minimum energy kink configurations would saturate the bound and satisfy the so-called BPS equation

$$\partial_\zeta \delta = \pm \sqrt{2(1 - \cos \delta) + \lambda(\cos 2\delta - 1)}. \quad (\text{IV.6})$$

It is easy to show that the solutions of above equation also satisfy the original equations of motion. The (anti)soliton solution of the BPS equation can be written as,

$$\delta(\zeta) \pm = \pi \pm 2 \tan^{-1}(\Lambda \sinh \Lambda \zeta), \quad (\text{IV.7})$$

where $\Lambda = \sqrt{1 - 2\lambda}$ is a real positive constant. It can be easily seen that for $\lambda = 0$, the above solution reduces to the usual sine-Gordon kink $\delta_{\text{SG}}(\zeta) = 4 \arctan e^{\pm \zeta}$.

The BPS energy bound for the (anti)soliton can be expressed as

$$\begin{aligned} E_{\text{BPS}} &= M_E \int_{\delta(-\infty)=0}^{\delta(\infty)=2\pi} d\delta \sqrt{2(1 - \cos \delta) + \lambda(\cos 2\delta - 1)} \\ &= \frac{M_E}{\sqrt{2\lambda}} \int_{-\sqrt{2\lambda}}^{\sqrt{2\lambda}} dt \sqrt{1 - t^2} \\ &= 1.88 M_E. \end{aligned} \quad (\text{IV.8})$$

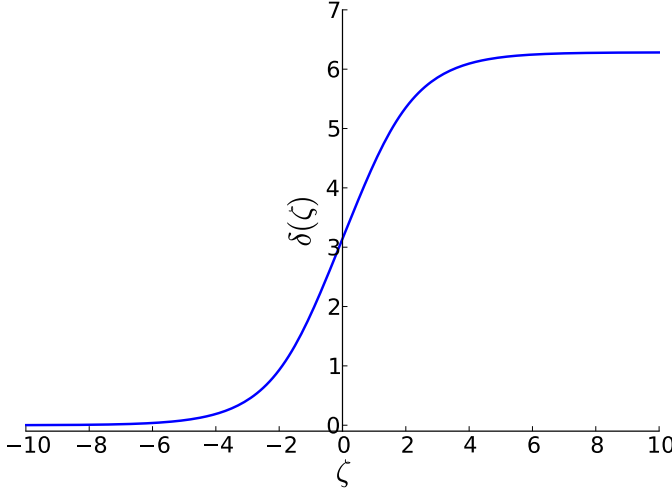


FIG. 4. The double sine-Gordon kink solution $\delta(\zeta)$ (IV.7) shown for $\Lambda = 0.813959$.

For a nuclear matter density of $\rho_n = 6 \times 10^{17} \text{ kg m}^{-3}$ [22] and a temperature of $T = 0.16 \text{ MeV}$ (as assumed in Appendix A and Table I), the total kink energy can be evaluated as

$$E_{\text{BPS}} = 93.3 \text{ MeV}. \quad (\text{IV.9})$$

We display in Fig. 4 the double sine-Gordon kink solution $\delta(\zeta)$ obtained for the λ values given in Eq. (III.5). In Fig. 5,

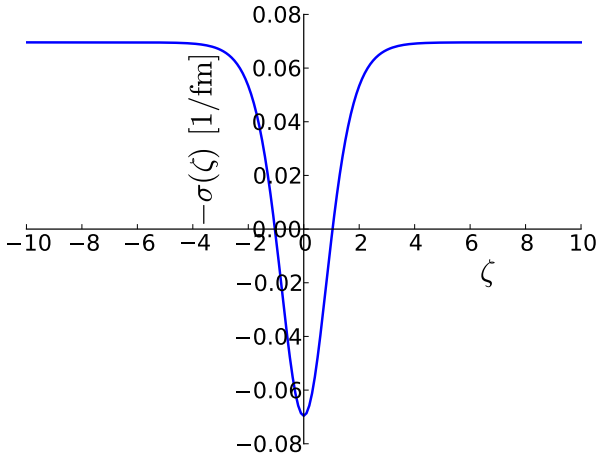


FIG. 5. The magnetization $\left(\frac{2m(\zeta)}{|\gamma_n|\hbar} = -\sigma(\zeta)\right)$ plotted as a function of the rescaled z -coordinate ζ .

we plot the change in the vortex core magnetization in the presence of the kink solution along the z -axis. When substituting (IV.7) in Eq. (II.15), it is observed that the magnetization

changes its value continuously and reaches its opposite value at the center of the kink.

Note that in this article we observed a sign flip of the trapped magnetic moment inside the core of a 3P_2 neutron superfluid vortex. For this case it is natural to think of the system as a chain of aligned magnetic moments with a flipped moment at the position of the kink. Hence, $\nabla \cdot \mathbf{M} \neq 0$ on the junctions, where \mathbf{M} is defined in Eq. (II.13). Since the total magnetic field \mathbf{B} is divergenceless, $\nabla \cdot \mathbf{B} = 0$, there would be a leakage of a magnetic field, say \mathbf{H} , from the junctions. In this case $\nabla \cdot \mathbf{H} \neq 0$ at the junctions and the total magnetic field is defined as $\mathbf{B} = (\mathbf{H} + 4\pi\mathbf{M})$. We schematically show in Fig. 6 an example of a magnetic field configuration with a flipped magnetic moment together with the resulting leakage of the magnetic field.

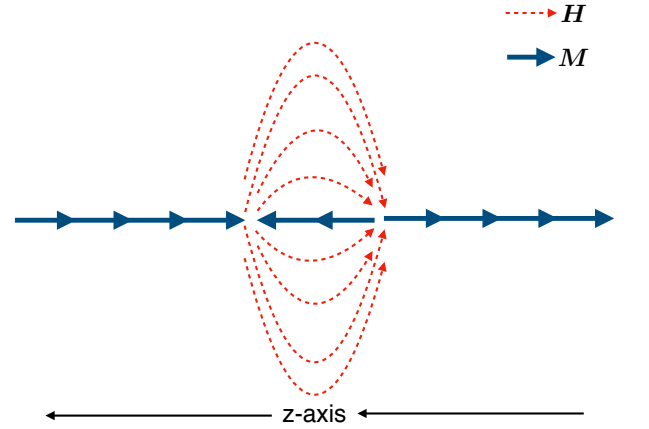


FIG. 6. A schematic figure of a magnetic field configuration to illustrate the flipped magnetic moment and the leakage. The dotted red arrows and the solid blue arrows denote the magnetic field \mathbf{H} and magnetic moment \mathbf{M} , respectively.

V. CONCLUSIONS

In this article, we have derived an effective theory of 3P_2 neutron superfluid vortices at large distances and expressed solely in terms of the phase δ of the vortex profile function g . g lives in one of the off-diagonal components of the tensorial 3P_2 order parameter $A_{\alpha i}$. Here, δ plays a crucial role as it gives a nonzero spontaneous magnetisation in the core region of 3P_2 neutron superfluid vortices for the angular independent profile function g . Variations in δ change the induced magnetic moment accordingly. In our analysis we have found

that at low energies the 3P_2 superfluid vortices are described by a double sine-Gordon model in addition to the well-known Kelvin (translational zero) modes part. We have derived a kink solution of this particular double sine-Gordon model and have determined its BPS energy bound. We have found that the vortex core magnetisation flips its direction at the kink on the vortex.

Since the number of vortices in a rotating NS is of the order of 10^{19} and the NS radius is about 10 km, there should exist a large number of magnetic strings in the NS interior like the ones discussed in this paper. A pair of kink and anti-kink may be created spontaneously during the creation of the vortex through phase transition. Possible implications of these objects for NS physics should be one of the most important future problems.

In this article, we have neglected higher order terms (esp. sixth order terms) in the GL free energy. We also did not take into account the effect of an external magnetic field. However, in the core of neutron stars where it is most likely to find neutron superfluid, the inclusion of high external magnetic fields and of the sixth order term would be important. So it would be interesting to study the effective free energy in the presence of high external magnetic fields and with nonzero sixth order term included. We have also considered only static configuration in this article. In order to discuss dynamics, we have to include time dependence. To this end, we need a time dependent GL equation, which has not been obtained yet. For the time-dependent problem, the phase δ has to be promoted to a time-dependent function and can be treated as a field which lies on the two-dimensional string world sheet. Fluctuations of δ may indicate changes in the magnetization on the world sheet. In the case of conventional superfluids, Kelvin modes will propagate with quadratic dispersion relation for small system sizes, see e. g. Ref. [51]. However, it is well known that for large system sizes the dispersion relation is given by $\varepsilon = k \log k$ with wave vector k . Recently, a formula for arbitrary system sizes has been obtained in Ref. [52]. On the other hand, the gapfull mode δ was previously unknown. We expect δ to have relativistic dynamics.

In this article, we have discussed only the integer vortex. For strong magnetic fields, the ground state is in the D_4 -biaxial nematic phase admitting half-quantized non-Abelian vortices [43]. The vortex core magnetization is ten times larger than that of the integer vortex. For this case we should also derive the low-energy collective coordinate approximation and construct a magnetic lump.

ACKNOWLEDGEMENTS

This work is supported by the Ministry of Education, Culture, Sports, Science (MEXT)-Supported Program for the Strategic Research Foundation at Private Universities “Topological Science” (Grant No. S1511006). C. C. acknowledges support as an International Research Fellow of the Japan Society for the Promotion of Science (JSPS). Some of the work of M. H. was undertaken at the Department of Mathematics and Statistics, University of Massachusetts, financially supported by FP7, Marie Curie Actions, People, International Research Staff Exchange Scheme (IRSES-606096). The work of M. N. is supported in part by JSPS Grant-in-Aid for Scientific Research (KAKENHI Grant No. 16H03984), and by a Grant-in-Aid for Scientific Research on Innovative Areas “Topological Materials Science” (KAKENHI Grant No. 15H05855) and “Nuclear Matter in Neutron Stars Investigated by Experiments and Astronomical Observations” (KAKENHI Grant No. 15H00841) from the the Ministry of Education, Culture, Sports, Science (MEXT) of Japan.

Appendix A: Ginzburg-Landau Description for 3P_2 Superfluids

In this appendix, we briefly discuss the Ginzburg-Landau (GL) construction of 3P_2 superfluids and the associated GL parameter values. The Hamiltonian with 3P_2 contact interaction can be written as

$$H = \int d^3\rho \, \psi^\dagger \left(-\frac{\nabla^2}{2M} - \mu \right) \psi - \frac{1}{2} g T_{\alpha\beta}^\dagger(\rho) T_{\alpha\beta}(\rho), \quad (\text{A.1})$$

$$T_{\alpha\beta}^\dagger(\rho) = \psi_\sigma^\dagger(\rho) (t_{\alpha\beta}^*)_{\sigma\sigma'}(\nabla) \psi_{\sigma'}^\dagger(\rho), \quad (\text{A.2})$$

where ρ denotes the space coordinates, ψ is a neutron field, μ is a baryon chemical potential, M is the neutron mass, and $g(>0)$ is the coupling constant. Here, α, β are the space indices, and the tensor $T_{\alpha\beta}$ represents the 3P_2 pair creation and annihilation operator. The differential operator t is defined as

$$(t_{\alpha\beta})_{\sigma\sigma'}(\nabla) = \frac{1}{2} ((S_\alpha)_{\sigma\sigma'} \nabla_\beta + \nabla_\alpha (S_\beta)_{\sigma\sigma'}) - \frac{1}{3} \delta_{\alpha\beta} (\mathbf{S})_{\sigma\sigma'} \cdot \nabla, \quad (\text{A.3})$$

and \mathbf{S} is given by $(S_\alpha)_{\sigma\sigma'} = i(\sigma_y \sigma_\alpha)_{\sigma\sigma'}$ with $\alpha = x, y, z$ and pauli matrices σ .

The 3P_2 order parameter can be represented in general as a 3×3 traceless symmetric complex tensor $A_{\mu i}$, which is defined in Refs. [42, 45] as

$$\Delta = \sum_{\alpha i} i \sigma_\alpha \sigma_y A_{\alpha i} k_i, \quad (\text{A.4})$$

where Δ is the gap parameter. As above, Greek subscripts stand for spin indices while Roman indices denote the spatial coordinates. The tensor $A_{\alpha i}$ is related to $T_{\alpha\beta}$ as given in Ref. [22],

$$A_{\alpha\beta} = g \langle T_{\alpha\beta}(\boldsymbol{\rho}) \rangle_T, \quad (\text{A.5})$$

where the angular brackets are defined as an ensemble average in the grand canonical ensemble.

Appendix B: The Large Distance Behaviour of the Order Parameter for a Vortex

An ansatz for the order parameter A of a vortex state has been developed first in Refs. [21, 22]. Here, we briefly sketch its derivation. For a detailed derivation we refer the interested reader to Ref. [46]. For an isolated vortex solution with cylindrical symmetry and phase $m\theta$, where m measures the circulation about the vortex line, we first choose the order parameter at large distances by minimising the potential in Eq. (II.3b) as

$$A \sim C(\eta) e^{im\theta} R(\theta) \begin{pmatrix} \eta & 0 & 0 \\ 0 & -(1+\eta) & 0 \\ 0 & 0 & 1 \end{pmatrix} R^T(\theta) \quad (\text{B.1})$$

$$C(\eta) = \sqrt{\frac{|\alpha|}{\beta(1+\eta^2 + (1+\eta)^2)}}.$$

Here $R(\theta)$ is the rotation matrix which rotates the axis from (ρ, θ, z) into (x, y, z) . Unlike in the case of the ground state, the order parameter can also have extra contributions from the kinetic terms in the free energy functional. Both the K_1 and K_2 terms in Eq. (II.3a) give logarithmic contributions to the total energy. Minimizing the coefficient of the logarithmic term breaks the ground state degeneracy for all $-1 \leq \eta \leq -\frac{1}{2}$ and the lowest energy is achieved for $\eta = 6 - \sqrt{43} \sim -0.557$. Hence, for a vortex configuration of minimal energy we may choose the matrix order parameter of a vortex state as given in Refs. [21, 22, 42, 46]

$$A \sim \sqrt{\frac{|\alpha|}{6\beta}} e^{i\theta} R(\theta) \begin{pmatrix} f_1 & 0 & 0 \\ 0 & f_2 & 0 \\ 0 & 0 & -f_1 - f_2 \end{pmatrix} R^T(\theta), \quad (\text{B.2})$$

where the boundary conditions for the profile functions are chosen according to the large distance behaviour in Eq. (B.2).

In Table I, we summarise the coefficients α , β , K_1 and K_2 (the GL parameters) calculated in the weak coupling limit

by considering only the excitations around the Fermi surface [22, 45, 46]. In this limit, K_1 and K_2 in Eq. (II.3a) take the same value. To simplify comparison with the works [22, 27, 42], the GL parameters are calculated for a nuclear mass density of $\rho_n = 6 \times 10^{17} \text{ kg m}^{-3}$ [22], Fermi momentum $k_F = 2.1987 \text{ fm}^{-1}$, nucleon mass $m_n = 0.02413 \text{ MeV}^{-1} \text{ fm}^{-2}$, a critical temperature for 3P_2 pairing of $T_C = 0.2 \text{ MeV}$ and a temperature of $T = 0.8 T_C$.

Appendix C: Equations of Motion

In this appendix, we list explicitly all the vortex equations together with the imposed boundary conditions. Note that all vortex equations are given in the cylindrical basis ($n = 1$).

The equations of motion derived from (II.11) are given by

$$\tilde{\rho}^2 (4u'' + v'') + \tilde{\rho} (4u' + 3v' - 4g') - (4u - v + 4g) - \frac{\tilde{\rho}^2}{144} \left(\frac{36\alpha}{|\alpha|} + 9u^2 + 3v^2 + 20g^2 \right) u = 0, \quad (\text{C.1a})$$

$$\tilde{\rho}^2 (u'' + 2v'') + \tilde{\rho} (2v' - u') - (10v - u - 16g) - \frac{\tilde{\rho}^2}{144} \left(\frac{12\alpha}{|\alpha|} + 3u^2 + v^2 + 12g^2 \right) v = 0, \quad (\text{C.1b})$$

$$4\tilde{\rho}^2 g'' + 2\tilde{\rho} (2g' + u') + 2(4v - u - 10g) - \frac{\tilde{\rho}^2}{72} \left(\frac{12\alpha}{|\alpha|} + 5u^2 + 3v^2 + 4g^2 \right) g = 0. \quad (\text{C.1c})$$

All profile function u , v and g are required to vanish at the origin. At spatial infinity we impose the following boundary conditions which are compatible to the above equations of motion

$$u^2 = (f_1 + f_2)^2 = \frac{6}{(\eta^2 + (1+\eta)^2 + 1)}, \quad (\text{C.2a})$$

$$v^2 = (f_1 - f_2)^2 = \frac{6(2\eta + 1)^2}{(\eta^2 + (1+\eta)^2 + 1)}, \quad (\text{C.2b})$$

$$u' = v' = g' = g = 0. \quad (\text{C.2c})$$

Hence, with the vortex boundary state selected to be given by the lowest energy state $\eta = -0.557$ (due to the fourth order term), the linear combinations $u = f_1 + f_2$ and $v = f_1 - f_2$ have to fulfill the boundary conditions $u(\infty) = 1.9956$ and $v(\infty) = 0.2275$.

α	$K_1 = K_2$	β
$\frac{T - T_c}{2T_c}$	$\frac{7\zeta(3)}{240M_n^2} \frac{N(0)G}{(\pi T_c)^2} k_F^4$	$\frac{7\zeta(3)}{60} \frac{N(0)G}{(\pi T_c)^2} k_F^4$
-0.1	1106.32 fm ²	2.57664 (MeV fm) ⁻²

TABLE I. Summary of the GL parameters computed in the weak coupling limit. We refer the reader to the last paragraph of section A for the numerical values of all model parameters used in our numerical simulations.

- The Hans Bethe Centennial Volume 1906-2006.
- [3] N. Chamel and P. Haensel, *Living Rev. Rel.* **11** (2008).
- [4] *Lecture Notes for the NATO Advanced Study Institute on Timing Neutron Stars*, NATO ASI Series C, Vol. 262 (Kluwer Academic Press, 1989) held in Cesme, Turkey.
- [5] D. Page, M. Prakash, J. M. Lattimer, and A. W. Steiner, *Phys. Rev. Lett.* **106**, 081101 (2011).
- [6] P. S. Shternin, D. G. Yakovlev, C. O. Heinke, W. C. G. Ho, and D. J. Patnaude, *Month. Not. Roy. Astr. Soc.* **412**, L108 (2011).
- [7] L. B. Leinson, *Phys. Lett.* **B741**, 87 (2015).
- [8] D. Pines, J. Shaham, and M. Ruderman, *Nature Phys.Sci.* **237**, 83 (1972).
- [9] T. Takatsuka and R. Tamagaki, *Prog. Theor. Phys.* **79**, 274 (1988).
- [10] G. Baym, C. Pethick, D. Pines, and M. Ruderman, *Nature* **224**, 872 (1969).
- [11] P. W. Anderson and N. Itoh, *Nature* **256**, 25 (1975).
- [12] M. Ruderman, *Astrophys. J.* **203**, 213 (1976).
- [13] D. Pines and M. Ali Alpar, *Nature* **316**, 27 (1985).
- [14] G. Baym and D. Pines, *Ann. Phys.* **66**, 816 (1971).
- [15] M. A. Alpar, H. F. Chau, K. S. Cheng, and D. Pines, *Astrophys. J.* **459**, 706 (1996).
- [16] G. Baym, C. Pethick, and D. Pines, *Nature* **224**, 673 (1969).
- [17] R. Tamagaki, *Prog. Theor. Phys.* **44**, 905 (1970).
- [18] M. Hoffberg, A. E. Glassgold, R. W. Richardson, and M. Ruderman, *Phys. Rev. Lett.* **24**, 775 (1970).
- [19] T. Takatsuka and R. Tamagaki, *Prog. Theor. Phys.* **46**, 114 (1971).
- [20] T. Takatsuka, *Prog. Theor. Phys.* **47**, 1062 (1972).
- [21] T. Fujita and T. Tsuneto, *Prog. Theor. Phys.* **48**, 766 (1972).
- [22] R. W. Richardson, *Phys. Rev.* **D5**, 1883 (1972).
- [23] N. D. Mermin, *Phys. Rev.* **A9**, 868 (1974).
- [24] J. A. Sauls and J. W. Serene, *Phys. Rev.* **D17**, 1524 (1978).
- [25] J. L. Song, G. W. Semenoff, and F. Zhou, *Phys. Rev. Lett.* **98**, 160408 (2007).
- [26] S. Uchino, M. Kobayashi, M. Nitta, and M. Ueda, *Phys. Rev. Lett.* **105**, 230406 (2010).
- [27] K. Masuda and M. Nitta, *Phys. Rev.* **C93**, 035804 (2016).
- [28] T. Mizushima, K. Masuda, and M. Nitta, *Phys. Rev.* **B95**, 140503 (2017), arXiv:1607.07266 [cond-mat.supr-con].
- [29] V. Z. Vulovic and J. A. Sauls, *Phys. Rev.* **D29**, 2705 (1984).
- [30] P. F. Bedaque, G. Rupak, and M. J. Savage, *Phys. Rev.* **C68**, 065802 (2003).
- [31] P. F. Bedaque and A. N. Nicholson, *Phys. Rev.* **C87**, 055807 (2013), [Erratum: *Phys. Rev.* **C89**, no.2, 029902 (2014)].
- [32] P. F. Bedaque, A. N. Nicholson, and S. Sen, *Phys. Rev.* **C92**, 035809 (2015).
- [33] L. B. Leinson, *Phys. Rev.* **C81**, 025501 (2010).
- [34] L. B. Leinson, *Phys. Lett.* **B689**, 60 (2010).
- [35] L. B. Leinson, *Phys. Rev.* **C82**, 065503 (2010), [Erratum: *Phys. Rev.* **C84**, 049901 (2011)].
- [36] L. B. Leinson, *Phys. Rev.* **C83**, 055803 (2011).
- [37] L. B. Leinson, *Phys. Rev.* **C84**, 045501 (2011).
- [38] L. B. Leinson, *Phys. Rev.* **C85**, 065502 (2012).
- [39] L. B. Leinson, *Phys. Rev.* **C87**, 025501 (2013).
- [40] K. M. Shahabasyan and M. K. Shahabasyan, *Astrophysics* **54**, 429 (2011).
- [41] P. Muzikar, J. A. Sauls, and J. W. Serene, *Phys. Rev.* **D21**, 1494 (1980).
- [42] J. A. Sauls, D. L. Stein, and J. W. Serene, *Phys. Rev.* **D25**, 967 (1982).
- [43] K. Masuda and M. Nitta, (2016), arXiv:nucl-th/1602.07050.
- [44] Sine-Gordon kinks on vortices were studied in the Skyrme model [56, 57]. In this case, the kink represents a Skyrmion, carrying a non-zero baryon number.
- [45] T. Fujita and T. Tsuneto, *Prog. Theor. Phys.* **49**, 371 (1973).
- [46] J. A. Sauls, *Anisotropic Superfluidity in Neutron Stars and Strong Coupling Effect in Superfluid ³He*, *Ph.D. Thesis, SUNY, Stony Brook*. (1980).
- [47] R. Barnett, A. Turner, and E. Demler, *Phys. Rev. Lett.* **97**, 180412 (2006).
- [48] S. Kobayashi, Y. Kawaguchi, M. Nitta, and M. Ueda, *Phys. Rev.* **A86**, 023612 (2012).
- [49] N. S. Manton, *Phys. Lett.* **B110**, 54 (1982).
- [50] M. Eto, Y. Isozumi, M. Nitta, K. Ohashi, and N. Sakai, *Phys. Rev.* **D73**, 125008 (2006).
- [51] M. Kobayashi and M. Nitta, *PTEP* **2014**, 021B01 (2014).
- [52] D. A. Takahashi, M. Kobayashi, and M. Nitta, *Phys. Rev.* **B91**,

- 184501 (2015).
- [53] R. J. Donnelly, *Quantized Vortices in Helium II*, Cambridge studies in low temperature physics (Cambridge University Press, New York, 1991).
- [54] E. B. Bogomolny, Sov. J. Nucl. Phys. **24**, 449 (1976), [Yad. Fiz. 24, 861 (1976)].
- [55] M. K. Prasad and C. M. Sommerfield, Phys. Rev. Lett. **35**, 760 (1975).
- [56] S. B. Gudnason and M. Nitta, Phys. Rev. **D90**, 085007 (2014).
- [57] S. B. Gudnason and M. Nitta, Phys. Rev. **D94**, 025008 (2016).